

Supplementary

Effects of interfacial transition layers on the electrical properties of individual $\text{Fe}_{30}\text{Co}_{61}\text{Cu}_9/\text{Cu}$ multilayered nanowires

Hongbin Ma,^{a†} Junwei Zhang,^{a†} Hong Zhang,^a Qianqian Lan,^a Chaoshuai Guan,^a Qiang Zhang,^b Feiming Bai,^c Yong Peng^{a*} and Xixiang Zhang,^{b*}

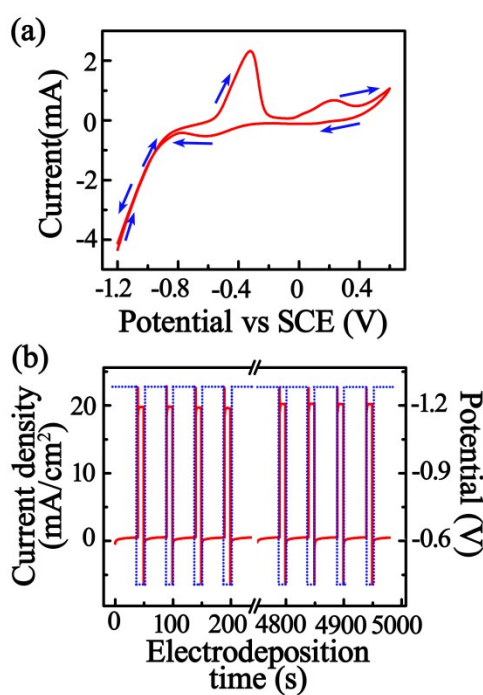


Fig. S1 (a) Cyclic voltammety recorded from a FeCo–Cu electrolytic solution used for the electrodeposition of multilayered $\text{Fe}_{30}\text{Co}_{61}\text{Cu}_9/\text{Cu}$ nanowires at a scanning rate of 10 mV/s. (b) Typical time-dependence curves of the applied deposition potential versus SCE (blue curve) and the observed current density (red curve) during the growth of $\text{Fe}_{30}\text{Co}_{61}\text{Cu}_9/\text{Cu}$ MNWs.

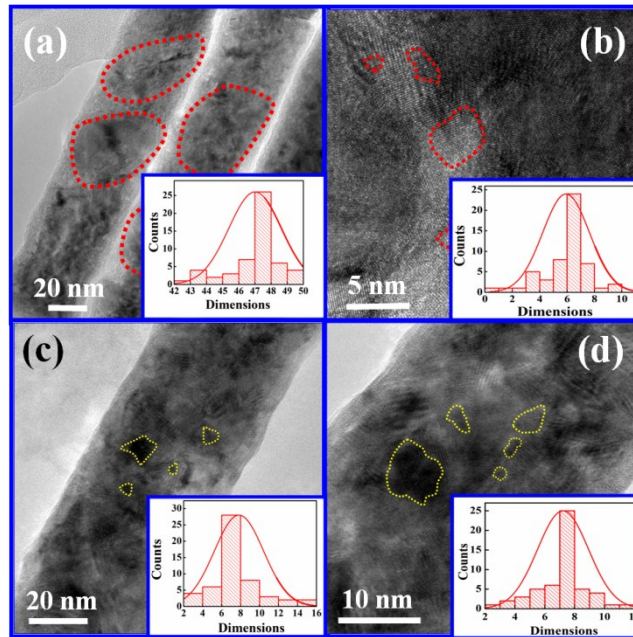


Fig. S2 HR-TEM images of grains inside a: (a) single-phase Cu nanowire; (b) Cu layer in a $\text{Fe}_{30}\text{Co}_{61}\text{Cu}_9/\text{Cu}$ MNW; (c) single-phase $\text{Fe}_{30}\text{Co}_{61}\text{Cu}_9$ nanowire; and (d) $\text{Fe}_{30}\text{Co}_{61}\text{Cu}_9$ layer in a $\text{Fe}_{30}\text{Co}_{61}\text{Cu}_9/\text{Cu}$ nanowire. Insets present the corresponding statistical grain size chart.

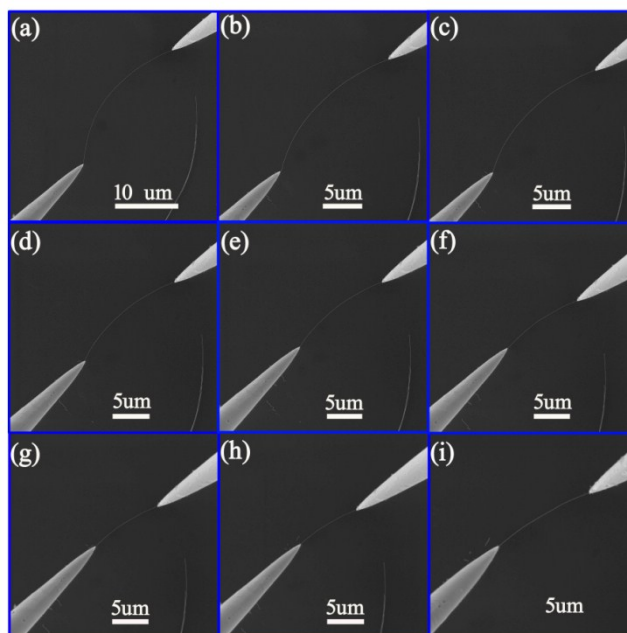


Fig. S3 SEM images of positions used to measure the resistance of single $\text{Fe}_{30}\text{Co}_{61}\text{Cu}_9/\text{Cu}$ MNWs; results were used to determine the R_7-L curve in Fig. 5 (a).

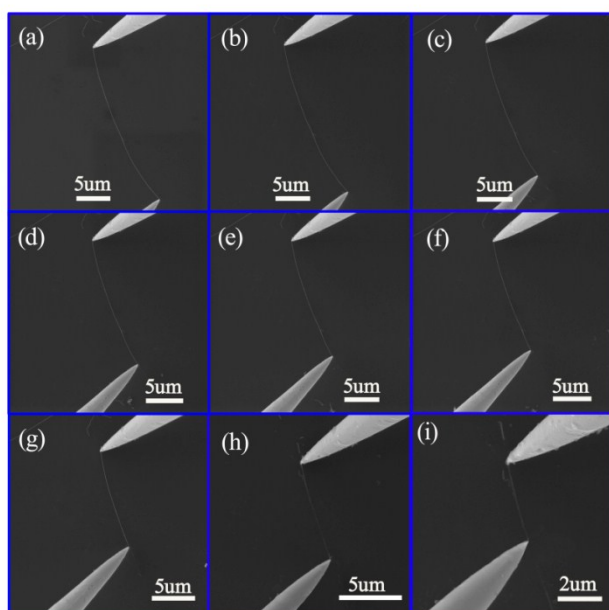


Fig. S4 SEM images of positions used to measure single-phase Cu nanowires, which were used to determine the R_c - L curve in Fig. 5b.

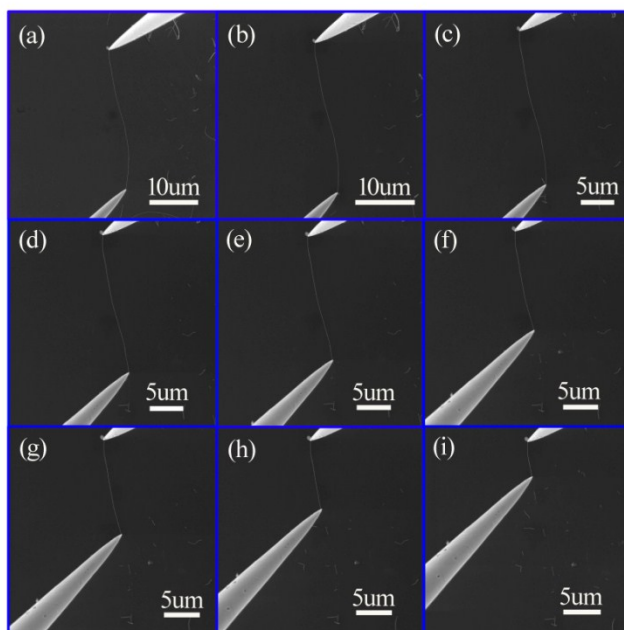


Fig. S5 SEM images of the positions used to measure single $\text{Fe}_{31}\text{Co}_{60}\text{Cu}_9$ nanowires, which were used to determine the R_L - L curve in Fig. 5f.